[4] Bandy, A. R., Hillard, M. E., and Emory, L. E., "Evaluation of Raman Scattering as a Sensor of Temperature and Molecular Density," *Applied Spectroscopy*, Vol. 27, No. 6, Nov./Dec. 1973, pp. 421–424.

Numerical Solution of Transonic Flows about Quasi-Cylindrical Configurations

ANTONIO FERRI,* SHELDON ELZWEIG,†
AND
PAOLO BARONTI‡
Advanced Technology Laboratories, Inc., Westbury, N.Y.

Introduction

NUMERICAL solutions of three-dimensional flows are lengthy and costly. A numerical algorithm is presented which allows for a fast solution of the transonic flow about quasi-cylindrical configurations of arbitrary shape. The method is conceptually similar to that developed by A. Ferri,[1] for conical flowfields without axial symmetry at supersonic speed.

Analysis

In order to describe the method, we consider the transonic small disturbance equation in terms of the perturbation potential and assume a configuration with one plane of symmetry. In a polar coordinate system, where the angle θ is zero in the vertical direction, the problem is described by the equation

$$[1-M_\infty{}^2-M_\infty{}^2(\gamma+1)\Phi_x]\Phi_{xx}+\Phi_{rr}+(1/r)\Phi_r = -(1/r^2)\Phi_{\theta\theta} \quad (1)$$

with the boundary condition, along a cylindrical surface $r = R$, $\phi_r(x, R, \theta) = (d/dx)r(x, \theta)$, where $r(x, \theta)$ has the general form

$$r(x, \theta) = \sum_0^n a_n(x)\cos n\theta \quad (2)$$

At infinity, the boundary condition is prescribed by either specifying the potential Φ or the proper normal Φ derivatives.

Express now the potential Φ as

$$\Phi(x, r, \theta) = \Phi_0(x, r)+\Phi_1(x, r)\cos\theta+\Phi_2(x, r)\cos 2\theta + \Phi_3(x, r)\cos 3\theta+\cdots \quad (3)$$

and rewrite Eq. (1) in the form

$$[1-M_\infty{}^2-M_\infty{}^2(\gamma+1)\Phi_x]\Phi_{xx}+\Phi_{rr}+(1/r)\Phi_r = (1/r^2)[\Phi_1\cos\theta+4\Phi_2\cos 2\theta+9\Phi_3\cos 3\theta+\cdots]$$

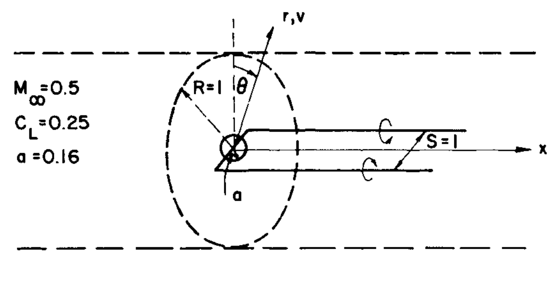

Fig. 1 Coordinates system and schematic of configuration.

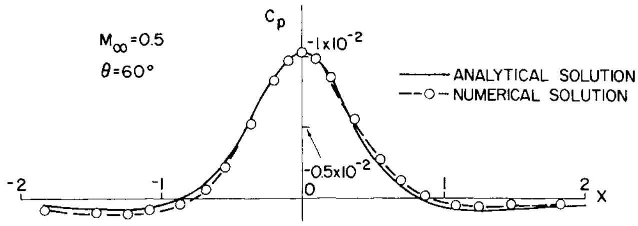

Fig. 2 Analytical and numerical solution of pressure distribution along a typical meridian plane.

This equation is then evaluated at selected θ_i planes so as to obtain the i equations

$$[1-M_\infty{}^2-M_\infty{}^2(\gamma+1)\Phi_x(x, r, \theta_i)]\Phi_{xx}(x, r, \theta_i)+\Phi_{rr}(x, r, \theta_i)+(1/r)\Phi_r(x, r, \theta_i) = (1/r^2)[\Phi_1\cos\theta_i+4\Phi_2\cos 2\theta_i+9\Phi_3\cos 3\theta_i+\cdots] \quad (4)$$

When the quantities $\Phi_1, \Phi_2, \Phi_3, \ldots$ are known, each equation, in each θ_i plane, corresponds to the usual two-dimensional transonic equation with a forcing term on the right-hand side and thus can be solved with any of the numerical schemes already developed for two-dimensional transonic flows. However, the quantities $\Phi_1, \Phi_2, \Phi_3, \ldots$ can be determined within the framework of the numerical relaxation procedures developed for the two-dimensional problem. Let us postulate that $\Phi_1, \Phi_2, \Phi_3, \ldots$ are those calculated at a preceding relaxation step, that is, $\Phi_1{}^{v-1}, \Phi_2{}^{v-1}, \Phi_3{}^{v-1}, \ldots$, where v indicates the previous iteration. Equation (4) can then be numerically solved in each θ_i plane at the vth iteration. Once this equation has been solved and the $\Phi_i{}^v(x, r, \theta_i)$ values determined, the Fourier expansion of Φ, Eq. (3), is written in the form

$$\Phi_i{}^v(x, r, \theta_i) = \Phi_0{}^v(x, r)+\Phi_1{}^v(x, r)\cos\theta_i + \Phi_2{}^v(x, r)\cos 2\theta_i+\Phi_3{}^v(x, r)\cos 3\theta_i+\cdots$$

and solved at the several θ_i planes to yield a system of i linear algebraic equations in the i unknowns $\Phi_0{}^v(x, r)$, $\Phi_1{}^v(x, r)$, $\Phi_2{}^v(x, r)$, $\Phi_3{}^v(x, r), \ldots$. These values are used for the solution of Eq. (4) in the subsequent iteration and the process continued until convergence. In conclusion, the solution of the transonic three-dimensional problem is reduced to the solution of i uncoupled two-dimensional transonic equations with a large reduction of computational time. The number i of two-dimensional equations to be solved is obviously equal to the number of terms that are retained in the Fourier series expansion of Φ. In turn, this number is dictated by the geometry of the body being considered, Eq. (2).

The solutions of the two-dimensional equations, in the θ_i planes, for both subcritical and supercritical conditions are obtained by a numerical program developed at Advanced

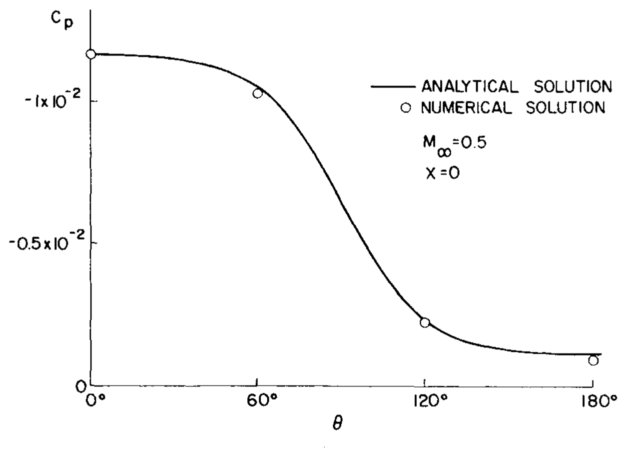

Fig. 3 Analytical and numerical solution of pressure distribution in a circumferential direction.

Received April 15, 1974; revision received June 3, 1974. This work is part of a continuing effort on wall corrections of transonic wind tunnels sponsored jointly by ONR and AFOSR under Contract N00014-72-C-0201. M. Cooper and M. Rogers are monitoring the work.

Index category: Subsonic and Transonic Flow.

* Technical Director; also Astor Professor, New York University. Fellow AIAA.

† Research Scientist.

‡ Senior Research Scientist. Member AIAA.

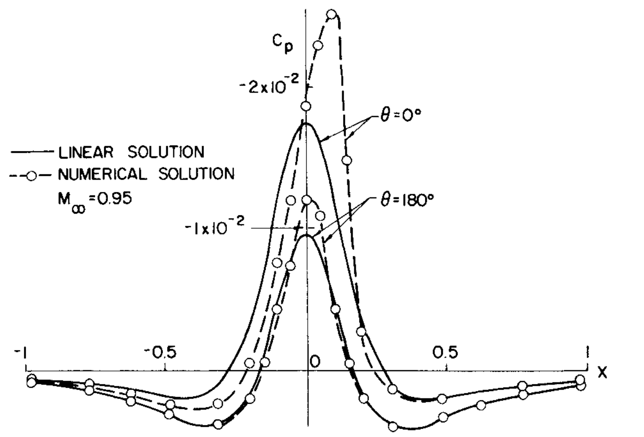

Fig. 4 Pressure distribution along typical meridian planes for supercritical conditions.

Technology Labs., Inc., and based on a modification of the method of Murman and Cole.[2] The modification, discussed in Ref. 3, consists in transforming the infinite domain around a two-dimensional shape into a finite one by the transformations $\xi = \tanh \alpha x$ and $\eta = 1 - e^{-\beta r}$, so that exact boundary conditions can be applied at the boundaries $\xi = \pm 1$ and $\eta = +1$, that is at the infinity of the physical plane. In the present case, the finite domain around a quasi-cylindrical surface is defined by $-1 \leq \xi \leq 1$ and ¶ $\leq \eta \leq 1$ where ¶ is the value of η for $r = R$.

Examples

To test the method, we have first compared a numerical solution with an exact analytical solution. We have computed analytically, using linear theory, the pressure coefficient and the velocity v induced along the cylindrical surface $r = R$ by the doublet-horseshoe vortex configuration shown in Fig. 1. Using as boundary condition along the surface $r = R$ the computed v (which, at any x can be shown to be adequately represented by four harmonics in θ) and using the potential induced by the horseshoe vortex as boundary condition at infinity around the cylinder, we have then solved numerically the linearized version of Eq. (4) along the four planes $\theta = 0°$, 60°, 120°, and 180°. Typical comparisons of C_p at $r = R$ are shown in Figs. 2 and 3. The numerical solution has converged after 200 iterations with a grid network of 41 × 20 points in each plane.

As a second step, a nonlinear, supercritical case has been analyzed numerically, by using as boundary condition at $r = R$ the Φ_y provided from linear theory by the same wing-body configuration of Fig. 1 with $M_\infty = 0.95$ and $C_L = 0.7$. At infinity around the cylinder, the boundary conditions that have been used are $\Phi_x = 0$ along the plane $x = \infty$ and $\Phi = 0$ everywhere else. By solving again Eq. (4) in the planes $\theta = 0°$, 60°, 120°, and 180°, the resulting pressure distributions at $r = R$ and along typical meridian planes are shown in Fig. 4 and compared with the analytical linear solutions. The supersonic pockets in the several meridian planes are shown in Fig. 5. Because of the courseness of the grid network that has been used (41 × 20 points) the supersonic region is identified by only a few grid points and the shock has been smeared through a relatively large region of the flow. A finer resolution could have been obtained with a finer mesh.

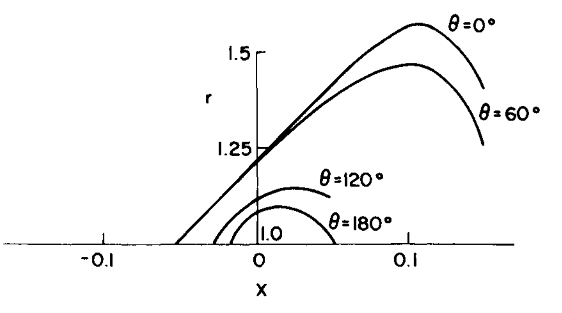

Fig. 5 Contour of supersonic region in several meridian planes.

It appears from these few examples that the method can be used advantageously to determine the flowfield around quasi-cylindrical shapes (lifting and nonlifting). Its application to other configurations, such as channel flows and flow around finite bodies without axial symmetry can also proceed in a similar manner. Similarly, the method can be extended to the complete nonlinear transonic equation with nonlinear boundary conditions.

References

[1] Ferri, A., "The Linearized Characteristic Method and Its Application to Practical Nonlinear Supersonic Problems," Rept. 1102, 1951, NACA.

[2] Murman, E. N. and Cole, J. D., "Calculation of Plane Steady Transonic Flows," *AIAA Journal*, Vol. 9, No. 1, Jan. 1971, pp. 114–121.

[3] Baronti, P., Elzweig, S., and Vaglio-Laurin, R., "Transonic Flows by Coordinate Transformation," *AIAA Journal*, Vol. 9, No. 11, Nov. 1971, p. 2280.

Photographic Observations of CW HF Chemical Laser Reacting Flowfield

R. L. Varwig*

The Aerospace Corporation, El Segundo, Calif.

Introduction

THE luminosity of the gas from the reaction $F + H_2 \rightarrow HF(v) + H$ in the reacting region of an HF chemical laser permits photographic observation of fluid dynamic flow phenomena. More extensive observations are presented in Ref. 1.

The triple-slit nozzle configuration described in Ref. 2 was used in this study (Fig. 1). The primary nozzle from which He and F atoms emerge is a wedge-shaped nozzle nominally 0.020 × 0.500 in. at throat cross section, 0.625 in. long, and 0.254 × 0.500 in. at exit cross section. H_2 fuel is injected from

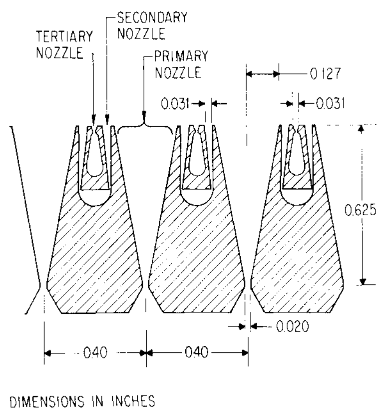

Fig. 1 Portion of the 16-nozzle triple-slit nozzle bank showing gas injection scheme.

Received May 6, 1974; revision received May 30, 1974. This work was supported by the U.S. Air Force under Contract F04701-73-C-0074. The author gratefully acknowledges helpful discussions with H. Mirels and W. R. Warren Jr.

Index categories: Reactive Flows; Lasers.

* Staff Scientist. Member AIAA.